Available online at www.sciencedirect.com
ScienceDirect
Journal of Catalysis 245 (2007) 456–465
JOURNAL OF CATALYSIS
www.elsevier.com/locate/jcat

Chemical and physical changes related to the deactivation of alumina used in catalytic epoxidation with hydrogen peroxide

Roberto Rinaldi, Fred Y. Fujiwara, Ulf Schuchardt *

Instituto de Química, Universidade Estadual de Campinas, PO Box 6154, 13083-970 Campinas, SP, Brazil

Received 3 October 2006; revised 7 November 2006; accepted 9 November 2006

Available online 6 December 2006

Abstract

This report addresses several questions regarding the deactivation of alumina in catalytic epoxidation using aqueous 70% H_2O_2. The structural, textural, morphological, and chemical changes of a polycrystalline alumina (γ-Al_2O_3 and boehmite) were studied in five consecutives reactions of 24 h. The chemical and physical processes involved in the transformations during alumina recycling are attributed mainly to the presence of water in the reaction mixture. Water plays a dual role in the catalytic system. On the one hand, water may cause deleterious changes of the structure of γ-Al_2O_3 and its textural properties. On the other hand, the presence of water shifts the adsorption equilibria of the organic molecules (acetic acid, diols, and oligomers), preserving the type Ia Al–OH sites, which are active for catalytic epoxidation. In this way, the water in the alumina/H_2O_2 catalytic system seems to be significant in prolonging the lifetime of the catalyst.

Keywords: Catalyst deactivation; Alumina; Epoxidation; Hydrogen peroxide; Solid-state NMR

1. Introduction

Catalytic deactivation is a phenomenon caused by a number of chemical and physical changes of a catalyst that result in decreased activity and/or selectivity. The causes of deactivation are classically divided into three categories: chemical, thermal, and mechanical [1,2]. Usually, catalyst stability is a challenge during liquid-phase oxidation due to (i) leaching of the active species into the reaction mixture; (ii) poisoning of the active sites by diols or carboxylates formed in the reaction; (iii) loss of chemical stability of the catalytic support; and (iv) the structural "stress" caused by the continuing change of oxidation number of the active metal sites and/or formation of oxometal sites in the matrix framework. Several heterogeneous catalysts for liquid-phase oxidations are in fact like Greek warriors in a Trojan horse, because small amounts of the active species are released into the solution, which are then responsible for their catalytic activity [3,4].

Alumina is an inexpensive and nonpolluting heterogeneous catalyst that efficiently catalyzes the epoxidation of a variety of nucleophilic alkenes, such as terpenes [5–7] and linear, cyclic, and functionalized olefins [5,8,9], using aqueous 70 wt% hydrogen peroxide or anhydrous 24 wt% H_2O_2 in ethyl acetate [10]. The ultrapure γ-Al_2O_3 obtained by the calcination of precursors synthesized by sol–gel routes showed significantly higher epoxidation activity compared to commercial chromatographic neutral alumina [11]. The surface hydrophilicity and the amount of weak to moderate Brønsted acid sites are among the responsible factors for the catalytic activity of aluminas [12–14]. In an earlier paper [15], we reported that using 70 wt% hydrogen peroxide instead of anhydrous 24 wt% H_2O_2 in ethyl acetate prolongs the lifetime of the catalyst. However, many questions on alumina deactivation and the role of water present in the reaction mixture could not be answered.

In this work, we address these pending questions by analyzing the structural, morphological, textural, and chemical transformations of the sol–gel alumina used in five consecutive cycles in catalytic *cis*-cyclooctene epoxidation with 70 wt% H_2O_2.

* Corresponding author. Fax: +55 19 35213023.
E-mail address: ulf@iqm.unicamp.br (U. Schuchardt).

0021-9517/$ – see front matter
doi:10.1016/j.jcat.2006.11.011

2. Experimental

2.1. Synthesis of the catalyst

The precursor of the calcined alumina, boehmite, was obtained by hydrolysis of aluminum *sec*-butoxide (Merck, 99.8%). In a 500-mL three-necked round-bottomed flask, 72.00 g of ultrapure water (Milli-Q) were added, under mechanical stirring, to 240.00 g of 50 wt% aluminum *sec*-butoxide in *sec*-butanol (Merck, p.a.). (CAUTION: THIS REACTION IS HIGHLY EXOTHERMIC!). The mixture obtained was stirred for 5 min, until it transformed into a homogeneous gelatinous slurry. This gel was placed on a rectangular glass plate (17 × 28 cm) and dried at 120 °C for 24 h, resulting in the xerogel. About 10.0 g of the xerogel were heated at a rate of 1 °C min^{-1} under a static air atmosphere to 200 °C, where the solid was maintained for 3 h, to 300 °C for another 3 h, and finally to 400 °C for 24 h, yielding the material designated as "cycle 0." The calcined alumina was stored in closed flasks in a desiccator over silica-gel and 3 Å molecular sieves for subsequent characterization and use in the catalytic epoxidation.

2.2. Catalytic reactions

2.2.1. Epoxidation of cis-cyclooctene

The aqueous solution of hydrogen peroxide (70 wt%) was supplied by Peróxidos do Brasil SA. (Solvay) and used without further treatment. The reaction mixture was prepared to contain 1.00 mol L^{-1} of *cis*-cyclooctene (Acros; 95%) and 0.500 mol L^{-1} of *n*-butylether (internal standard; Acros; >99%) in ethyl acetate (Merck; p.a.).

To a two-necked round-bottomed flask containing 20 mL of the reaction mixture (20.0 mmol of cyclooctene and 10.0 mmol of *n*-butylether), 2.00 mL (56 mmol) of aqueous 70 wt% H_2O_2 solution was added. The mass of the reaction mixture was determined for calculating the hydrogen peroxide content. This mixture was heated to 80 °C with magnetic stirring. An initial aliquot ($t = 0$ h) was taken for gas chromatography (GC) analysis, and the reaction was started by addition of the alumina (200.0 mg). A final aliquot (50 μL) was taken after 24 h. Both aliquots were diluted in hexane (2 mL; Tedia; HPLC grade), treated with a few milligrams of manganese dioxide to promote decomposition of the peroxides and then with anhydrous sodium sulfate to remove residual water. These solutions were analyzed using a Hewlett-Packard HP 5890 series II gas chromatograph equipped with an Alltech AT-WAX capillary column (20 m × 0.25 mm × 0.25 μm film thickness) and a flame ionization detector. The *cis*-cyclooctene epoxide was quantified using a calibration curve obtained with a standard solution. Selectivity is always given with respect to converted *cis*-cyclooctene.

2.2.2. Catalyst recycling

In the first cycle, eight reactions were carried out in parallel to ensure sufficient catalyst for recycling experiments and catalyst characterization. The catalyst was used five times and aliquots were taken after the first, third, and fifth cycles for characterization. For each catalyst recycling, the alumina was filtered off from the reaction mixture and washed with three portions (50 mL) of ethyl acetate (Merck; p.a.) at room temperature. The alumina powders from the same cycle were mixed and dried at 130 °C for 24 h. After this treatment, the catalyst samples after use in the first, third, and fifth cycles (herein designated as "cycle 1," "cycle 3," and "cycle 5") were stored in closed flasks in a desiccator over silica-gel and 3 Å molecular sieves for subsequent characterization and/or reuse.

2.2.3. Determination of hydrogen peroxide

To an Erlenmeyer flask, 50 mL of aqueous 20 wt% acetic acid and 20 g of dry ice for deaeration of the solution were added. After 2 min, ca. 2.0 g of potassium iodide (Synth; p.a.) and 3 drops of a 1-wt% ammonium molybdate solution (Vetec; p.a.) were added. To this mixture, a 200 mg aliquot of the reaction mixture, collected before and after the reaction (0 and 24 h), was added. The iodine formed was titrated with a 0.1 mol L^{-1} solution of sodium thiosulfate (Synth; p.a.). Near the endpoint of the titration (pale brown color), 1.0 mL of a 1 wt% starch solution was added. The endpoint was detected when the blue color disappeared. The amount of H_2O_2, $n_{H_2O_2}$, (in mmol) in the reaction mixture was calculated by

$$n_{H_2O_2} = \frac{C_{S_2O_3^{2-}} \cdot V_{S_2O_3^{2-}}}{2} \cdot \frac{m_{\text{reaction}}}{m_{\text{aliquot}}} \cdot 10^3, \quad (1)$$

where $C_{S_2O_3^{2-}}$ is the concentration of the sodium thiosulfate solution (mol L^{-1}), $V_{S_2O_3^{2-}}$ is the volume of sodium thiosulfate solution (L), m_{reaction} is the mass of the reaction mixture (g), and m_{aliquot} is the mass of the aliquot (g) taken after 0 and 24 h. To determine the H_2O_2 content after 24 h, the alumina mass was included in the mass of the reaction mixture.

2.3. Catalyst characterization

2.3.1. X-ray power diffraction

Powder X-ray diffraction (XRD) patterns were determined with a Shimadzu XD-3A diffractometer, using Cu$K\alpha$ radiation and 2θ of 5°–100°, with a step size of 0.02° and a counting time of 3 s. The phase identification was done using the PCPDFWIN v. 2.0 program and the crystallographic pattern files [21-1307] and [47-1308] for boehmite and γ-Al_2O_3, respectively.

2.3.2. Surface area analysis

The nitrogen adsorption–desorption isotherms were measured on a Micrometrics ASAP 2010 equipment. The samples were degassed at 120 °C under vacuum (1 μbar) for 3 h. The surface area was determined by adsorption–desorption of nitrogen at 77 K. The pore volume and average pore diameter were calculated using the BET method. The pore-diameter distributions were calculated using the BJH method on the desorption branch.

2.3.3. Scanning electron microscopy

Secondary electron images were acquired in a JEOL JSM 6360 LV scanning electron microscope, operating at 20 kV. The

samples were placed on brass stubs and coated with carbon followed by a gold–palladium (80%/20%) coating using a Bal-Tec MD 020 instrument (20 s and 30 μA).

2.3.4. MAS NMR analyses

The ^{27}Al, ^{1}H, and ^{13}C MAS NMR spectra were recorded using a Varian INOVA 500 spectrometer equipped with a 4-mm high-speed probe (Doty Scientific) at a spinning rate of 13 kHz. For the ^{27}Al MAS NMR spectra, the ^{27}Al chemical shifts were referenced to a 1.0-mol L^{-1} $Al(NO_3)_3$ solution. The experimental conditions were operating frequency of 130.26 MHz, acquisition time of 5 ms, pulse-width of 2.4 μs ($\pi/2$), recycle delay of 0.1 s, and spectral width of 32.2 kHz. For each spectrum, 2400 scans were acquired. The FIDs were processed using an exponential function with a line width of 1 Hz. The spectra were simulated using the OriginPro 7.5 (Originlab). For the ^{1}H MAS NMR spectra, the ^{1}H chemical shifts were referenced to water. The experimental conditions were operating frequency of 499.89 MHz, acquisition time of 50 ms, pulse width of 3.0 μs ($\pi/2$), recycle delay of 5.0 s, spectral width of 200.0 kHz. For each spectrum, 16 scans were acquired. The FIDs were processed using an exponential function with a line width of 0.1 Hz. For the $^{1}H \rightarrow {}^{13}C$ CP-MAS NMR spectrum of the cycle 5 alumina, the ^{13}C chemical shifts were referenced to adamantane, whereas the Hartmann–Hahn match was set also using adamantane. The experimental conditions were an operating frequency of 125.7 MHz, acquisition time of 50 ms, pulse width of 4.1 μs ($\pi/2$), recycle delay of 3.0 s, contact time of 2.5 ms, and spectral width of 50.0 kHz. For each spectrum, 7200 scans were acquired. The FIDs were processed using an exponential function with a line width of 12 Hz.

2.3.5. Fourier transform infrared spectroscopy

The FTIR spectra were recorded using 64 scans between 400 and 1600 cm^{-1} in a Bomen IR spectrometer MB series from Hartmann and Braun with a resolution of 4 cm^{-1}. Analyses were performed from samples (1 wt%) ground together with KBr.

2.3.6. Thermogravimetric analysis

Thermogravimetric analysis (TGA) was carried out under an oxidative atmosphere (synthetic air, 100 mL min^{-1}) using a TA Micrometrics 2950 TGA instrument with a heating rate of 20 °C min^{-1} in the range of 30–900 °C. The analyses were performed in duplicate for each sample.

2.3.7. Elemental analysis

Elemental analyses were carried out using a Perkin-Elmer Series II CHN S/O analyzer model 2400. The alumina samples were mixed with an oxidant mixture (Pb_3O_4/NaF, 1:7) and the elemental analyses were performed by combusting the samples at 925 °C. The analyses were done in triplicate.

2.3.8. Measurements of pH of the aqueous suspension of catalyst

The pH of the aqueous suspensions of the unused and used catalyst (solid-to-liquid ratio of 5 g L^{-1}) was measured under an argon atmosphere at 25 °C using a pHmeter (Quimis) equipped with a combined glass electrode. The electrode was calibrated with three standard buffer solutions (pH 4, 7, and 10; Synth). The pH was recorded when the variation was $< \pm 0.05$ pH h^{-1}. To find out the presence of desorbed acetate in the solution, the suspension was centrifuged for 15 min at 10,000 rpm, and the clear supernatant was analyzed using an Agilent 8453 UV-Vis spectrometer.

3. Results and discussion

Alumina calcined at 400 °C is an efficient epoxidation catalyst for *cis*-cyclooctene with 70 wt% H_2O_2, yielding ca. 87% of epoxide with a selectivity of ca. 98% after 24 h and 1.6 mmol of H_2O_2 per mmol of epoxide formed was consumed (Table 1). The reaction without catalyst yielded ca. 10% of epoxide after 24 h and used 1.1 mmol of H_2O_2 per mmol of epoxide formed. The catalyst slowly lost its activity in the consecutive cycles, showing a moderate epoxide yield (ca. 65%) in the fifth cycle. The catalytic system alumina–aqueous H_2O_2 (70 wt%) showed an overall productivity of ca. 41 g of cyclooctene oxide per g of alumina. Although there was no statistical loss of selectivity for epoxide, the H_2O_2 consumption per epoxide formed increased after the fourth cycle from ca. 1.6 to 2.0. Between each cycle, the used alumina was washed with ethyl acetate and dried at 130 °C for 24 h to avoid structural and textural changes that could disguise the real changes occurring during the catalyst recycling experiments. Furthermore, it is known that recalcination of used commercial chromatographic alumina (Fluka, type 507C, neutral, 100–125 mesh) is unable to regenerate the initial catalytic properties of the alumina [11].

The catalyst is a mixture of γ-Al_2O_3 and pseudo-boehmite (Fig. 1), the pseudo-boehmite content was ca. 22 wt% (estimated from the TGA curve using the weight loss between 340 and 470 °C, which is assigned mainly to water evolved in the phase transition of pseudo-boehmite $\rightarrow$ γ-Al_2O_3 [16]). Catalyst recycling results in growth of a halo between 10° and 55°, indicating that part of the initial crystalline structure is lost when the catalyst is reused. It was recently reported that the aging of aqueous suspensions of γ-Al_2O_3 at room temperature for prolonged periods (weeks to months) resulted in the transformation of γ-Al_2O_3 into bayerite [β-$Al(OH)_3$] through an amorphous intermediate [17]. In the XRD patterns (Fig. 1), the presence of bayerite was not detected even after extended

Table 1
Catalytic results of the alumina recycling experiments on cyclooctene epoxidation with 70 wt% H_2O_2

Cycle	n[a]	Yield (%)	Selectivity (%)	Consumption of H_2O_2 (mmol of H_2O_2 per mmol of epoxide)
1	8	87 ± 4	97.6 ± 0.6	1.6 ± 0.1
2	6	81 ± 7	98.5 ± 0.9	1.5 ± 0.1
3	5	76 ± 5	97.8 ± 0.7	1.5 ± 0.1
4	3	73 ± 4	98.4 ± 0.3	1.6 ± 0.2
5	2	65 ± 6	96.8 ± 0.5	2.0 ± 0.1

[a] n is the number of parallel reactions carried out. Reaction conditions: 20 mmol of *cis*-cyclooctene, 10 mmol of di-*n*-butylether, 56 mmol of (70 wt%) H_2O_2 and 200.0 mg of alumina; 80 °C; 24 h.

catalyst use (5 days). However, the pseudo-boehmite reflections slightly increase their intensities for recycled catalyst. In fact, bayerite formation is reported to be less favored than boehmite formation in the temperature range used in the catalytic epoxidations [18,19].

With respect to the morphology of the surface particles, the unused catalyst looks like flakes of microspheres (cycle 0, Fig. 2). On recycling the catalyst, these microspheres coalesce, and the surface becomes flatter. After the fifth cycle, several small holes in the surface are found (cycle 5, Fig. 2), which may be formed by the O_2 evolved from the internal surface by decomposition of H_2O_2.

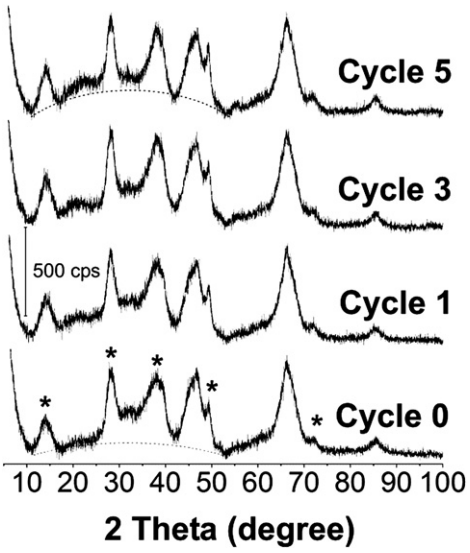

Fig. 1. XRD Patterns for the unused (cycle 0) and used catalyst (cycles 1, 3, and 5). (⋆) Indicate the boehmite reflections and the dotted curves (cycles 0 and 5) indicate the amorphous halos.

Table 2 shows the changes of textural properties of the alumina surface during the recycling experiments. The surface area, average pore diameter, and volume show more significant decreases after the first cycle of the catalyst than in the subsequent recyclings. The pore system is also constantly altered during the recycling experiments (Fig. 3). Initially, the catalyst pore system was formed by nonstructural slits due to particle packing (type II isotherm, hysteresis H3), which are slowly transformed into ink bottle-like pores (type IV isotherm, hysteresis H2). The pore diameter distribution curves (Fig. 4) also indicate that smaller pores are created during catalyst recycling.

Previous studies [6,13,14] showed that γ-Al_2O_3 with nonstructural pores, formed by slits between the particles (isotherm II, hysteresis H3) and having an open pore structure, show better performance in the alumina-catalyzed epoxidation. In addition, aluminas with ink bottle-like pores (type IV isotherm, hysteresis H2), are less active due to diffusion prob-

Table 2
Textural properties of the unused (cycle 0) and used catalyst (cycles 1, 3, and 5)

Cycle	A_{BET} ($m^2\ g^{-1}$)	Pore diameter (nm)	Pore volume ($cm^3\ g^{-1}$)
0	367	22.1	2.1
1	326	19.1	1.6
3	325	17.6	1.5
5	313	15.7	1.3

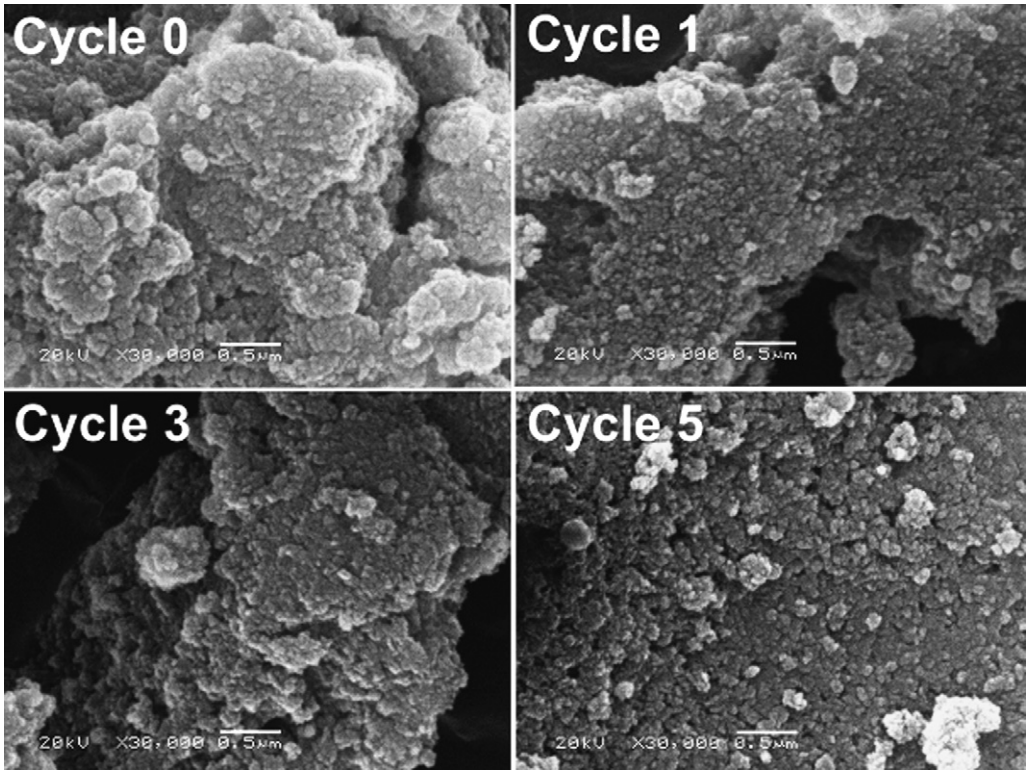

Fig. 2. SEM images for the unused (cycle 0) and used catalyst (cycles 1, 3, and 5). The white bar corresponds to 0.5 μm and the micrograph magnification is 30,000×.

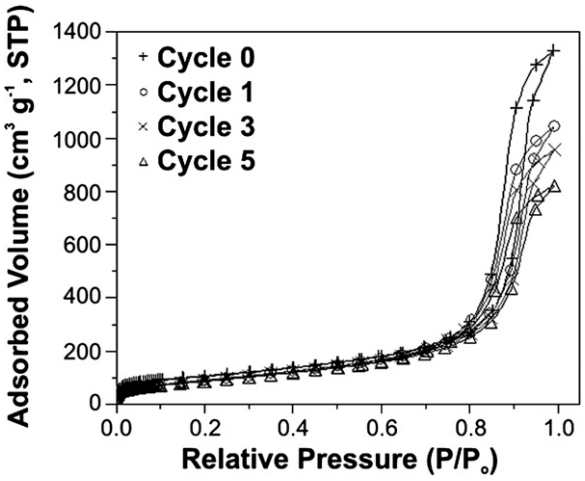

Fig. 3. Nitrogen adsorption–desorption isotherms at 77 K for the unused (cycle 0) and used catalyst (cycles 1, 3, and 5).

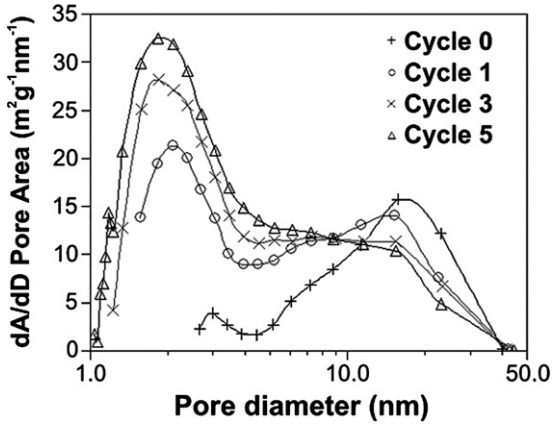

Fig. 4. Distribution of pore diameter calculated for the desorption branch of the nitrogen isotherms at 77 K for the unused (cycle 0) and used catalyst (cycles 1, 3, and 5).

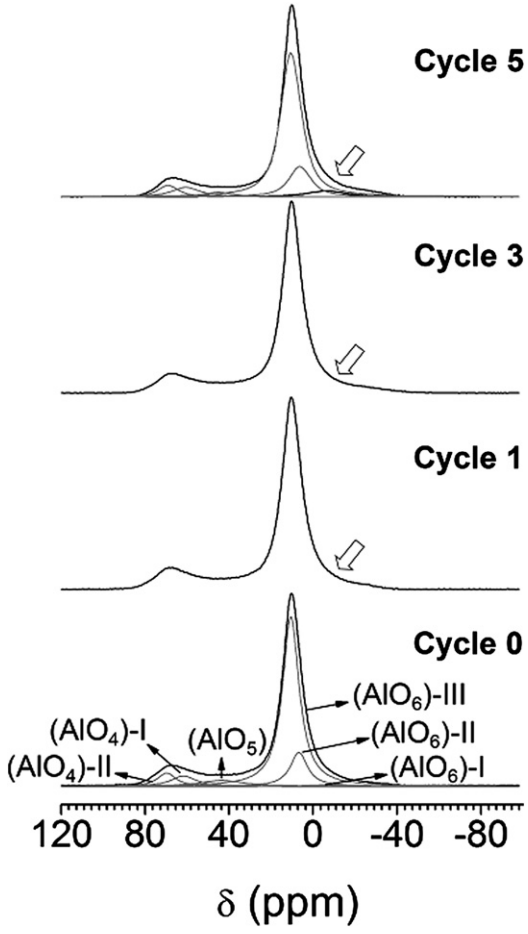

Fig. 5. ^{27}Al MAS NMR spectra for the unused (cycle 0) and used catalyst (cycles 1, 3, and 5). Arrows show the shoulder attributed to a broad resonance centered around −6 ppm, (AlO_6)-I (see lower broad black line in spectrum of catalyst cycle 5).

lems of the olefin through the hydrophilic pores, as well as being less selective in the epoxidation of highly reactive olefins, because the residence time of reagents and products inside these pores can be sufficiently long for further oxidation or ring-opening reactions [6]. Earlier, we reported that the higher activity of γ-Al_2O_3 with nonstructural pores was due to avoiding the entrapment of water in the porous system, which would make diffusion of the olefin to the active sites more difficult [14]. However, the present results provide new information on the increase of population of smaller pores when the catalyst is recycled (Fig. 4), which surely makes the diffusion of the olefin through the pore system more difficult. Therefore, this increase of population of smaller pores is a detrimental textural change to catalyst performance (activity and selectivity). ^{27}Al MAS NMR experiments were carried out to obtain more details on the structural transformations that happen during catalyst recycling (Fig. 5).

In the ^{27}Al MAS NMR spectra, at least four resonances are clearly present due to the AlO_6 (10 ppm), AlO_5 (50 ppm), and AlO_4 (60 and 70 ppm) sites. However, a broad shoulder centered in the region of −6 ppm, (AlO_6)-I, is discerned after consecutive catalyst recycling (Fig. 5). The resonance around 10 ppm assigned to the six-coordinated Al(III) ion is expected to comprise two signals, (AlO_6)-II and (AlO_6)-III, corresponding to the AlO_6 sites from boehmite and γ-Al_2O_3, respectively [20]. Two populations of four-coordinated Al(III) ion exist in the bulk structure; these are assigned to resonances around 60 and 70 ppm, (AlO_4)-I and (AlO_4)-II, respectively, related to the γ-Al_2O_3 structure. Based on these arguments, the fitting of six signals in the simulation of the ^{27}Al MAS NMR spectra was done. The estimated parameters of the ^{27}Al MAS NMR spectra are shown in Table 3.

The ^{27}Al nucleus ($I = 5/2$) has a quadrupolar moment that allows it to interact with any electric field gradient originating from distortions in the geometry of the Al(III) coordination sphere, which may result in broad resonance lines due to second-order quadrupolar interaction and may make highly distorted sites “invisible” to ^{27}Al MAS NMR spectroscopy [21,22]. However, for aluminas [20], this problem is minimized or even avoided using high magnetic fields, thereby taking advantage of the inverse proportionality of the second-order quadrupole interaction with the magnetic field and also of the increase in chemical shift dispersion [23].

Table 3
Estimated parameters for the AlO_x sites of simulated and fitted ^{27}Al MAS NMR spectra of the unused (cycle 0) and used catalyst (cycles 1, 3, and 5)

Cycle	Amorphous phase (AlO_6)-I			Boehmite (AlO_6)-II			γ-Al_2O_3											
							(AlO_6)-III			AlO_5			(AlO_4)-I			(AlO_4)-II		
	δ (ppm)	w (Hz)	%	δ (ppm)	w (Hz)	%	δ (ppm)	w (Hz)	%	δ (ppm)	w (Hz)	%	δ (ppm)	w (Hz)	%	δ (ppm)	w (Hz)	%
0	−6	2450	1	7	1280	14	11	1250	66	44	3400	6	62	1920	6	70	1410	6
1	−7	2610	2	7	1470	13	11	1330	67	44	3250	5	62	2040	7	70	1500	6
3	−7	6170	7	7	1440	14	11	1260	63	45	3140	5	61	1910	6	69	1430	5
5	−6	4280	9	7	1370	19	11	1180	57	46	2630	4	61	1850	5	69	1290	6

The broadest signal, (AlO_6)-I, ($w \sim 4$ kHz) is expected to be related to a kind of amorphous aluminum trihydroxide formed during the recycling experiments (Table 3). The relative amount of (AlO_6)-I sites increases after consecutive catalyst recycling from 2 to 9% (Table 3), which is in agreement with the higher intensity of the amorphous halo in the XRD patterns of recycled alumina (Fig. 1). The relative amount of (AlO_6)-II, which is assigned to AlO_6 bulk sites of boehmite, corresponding to a boehmite content of 17 wt% in the initial sample, is in good agreement with the value determined using the TG curve (22 wt%). In addition, the relative amount of (AlO_6)-II sites also gradually increases for more recycled alumina, whereas the relative populations of the (AlO_6)-III, AlO_5, and (AlO_4)-I sites, assigned to γ-Al_2O_3, decrease. These results suggest that during catalyst recycling, γ-Al_2O_3 is converted to boehmite and an amorphous aluminum trihydroxide (Fig. 4). These phase transformations may be related to the deactivation of calcined alumina, because boehmite is clearly less active than γ-Al_2O_3 and other transition polymorphs [9,13]. In addition, the formation of boehmite and/or an amorphous aluminum trihydroxide is potentially related to the increase of the population of smaller pores, because these materials typically have smaller mesopores or even micropores [18].

Another important factor for catalyst deactivation is the chemisorption of molecules that poison the active sites [1,2]. The FTIR spectra of the unused catalyst (cycle 0) and used catalyst (cycles 1, 3, and 5) show many bands between 1370 and 1600 cm^{-1} (Fig. 6), which are assigned to the formation of superficial carboxylates in many coordination modes [24]. In addition, a weak band at 1027 cm^{-1}, discerned for the used catalyst, is normally assigned to δ(Al–OH) of aluminum trihydroxides [25], which is a confirmation of the formation of an amorphous aluminum trihydroxide during the recycling experiments. The hydroxyl region of the FTIR spectra was omitted in Fig. 6 because only a broad band could be observed due to the strong IR absorption of adsorbed water on the alumina surface (see the full spectra in supplementary materials). Due to problems in preparing samples without modifying them, neither FTIR or Raman spectroscopy was able to provide semiquantitative information on changes of hydroxyls on the γ-Al_2O_3 surface. However, the intensities of the Raman lines assigned to boehmite were strongly enhanced (see supplementary materials) for the used catalyst (cycle 5), indicating that the catalyst surface is being recovered by boehmite crystallites (in agreement with the XRD powder patterns and ^{27}Al MAS NMR spectra). This fact corroborates with the hypothesis that the decrease

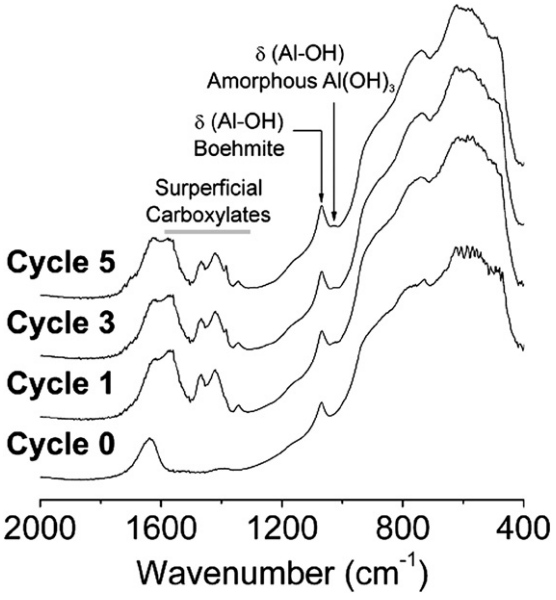

Fig. 6. FT-IR spectra for the unused (cycle 0) and used catalyst (cycles 1, 3, and 5).

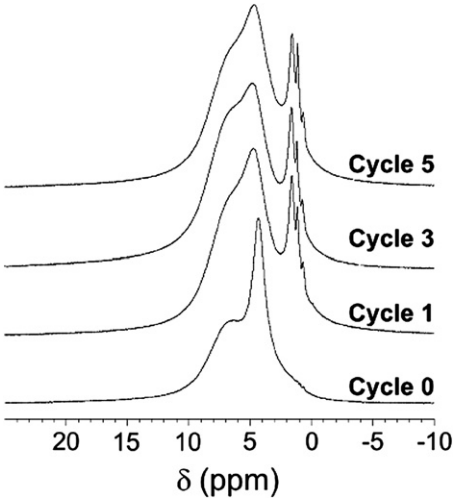

Fig. 7. ^1H MAS NMR spectra for the unused (cycle 0) and used catalyst (cycles 1, 3, and 5).

of catalytic activity is also caused by the formation of lesser active (oxy)-hydroxide aluminum phases [9,13], due to the reactions of γ-Al_2O_3 with water [17].

The ^1H MAS NMR spectra of used catalysts (Fig. 7) show three narrow resonances between 1 and 3 ppm. This observa-

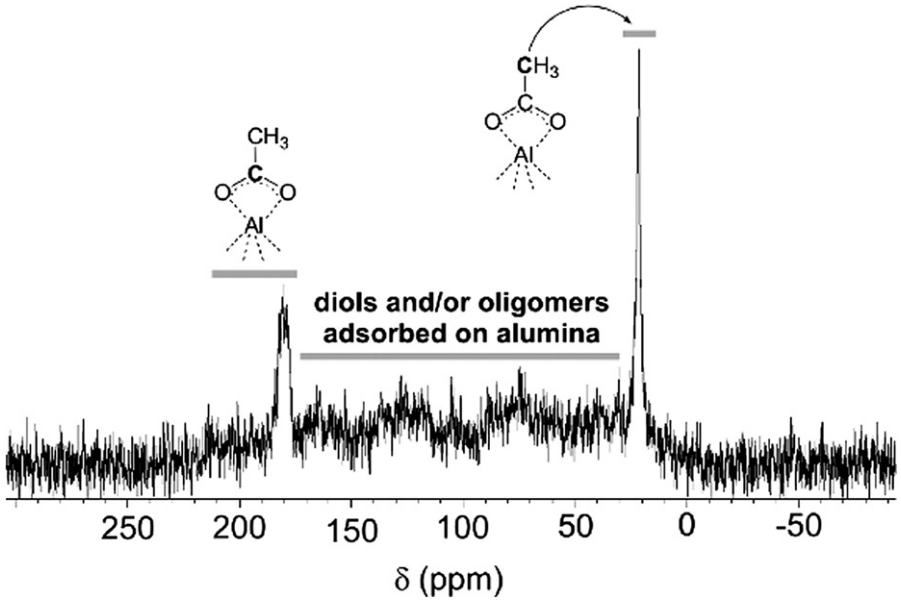

Fig. 8. $^{1}H \rightarrow {}^{13}C$ CP-MAS NMR spectrum for a used alumina (cycle 5).

tion is interesting, because no further information other than broad resonances is usually expected for unused alumina due to the very strong ^{1}H–^{1}H dipolar coupling (cycle 0, Fig. 7). The unused catalyst shows only a coalesced resonance at 6.5 ppm, assigned to Al–OH groups, and another at 4.6 ppm assigned to physisorbed water. Because molecular movement is restricted in the solid state, the overall dipolar coupling is large, which broadens the signals [21]. Consequently, the "narrow" resonances in the range of 1–3 ppm are related to groups with a high degree of freedom, such as the methyl groups. These methyl groups are attributed to acetate groups bonded to the alumina surface that originate from ethyl acetate hydrolysis and/or its direct reaction with loosely bonded hydroxyl groups on the alumina surface [12].

It is possible to have a more comprehensive idea of the molecules adsorbed on the alumina surface during the recycling experiments using $^{1}H \rightarrow {}^{13}C$ CP MAS NMR (Fig. 8). The signal intensities of the $^{1}H \rightarrow {}^{13}C$ CP MAS NMR spectrum are related not only to the amount of species adsorbed on the surface, but also to the efficiency of cross-polarization transfer. Therefore, these intensities should not be interpreted in a quantitative manner [21]. As shown in Fig. 8, other signals than those assigned to acetates bonded to the alumina surface can be seen in the range of 20–180 ppm and are assigned to other organic species on the alumina surface, such as diols and/or oligomers of cyclooctene oxide. These molecules are formed by acid-catalyzed epoxide ring opening. However, because cyclooctene oxide is relatively resistant to ring opening, there is no substantial loss of selectivity in the reactions (Table 1). On the other hand, for very sensitive epoxides, such as terpene epoxides, the selectivity and the mass balance of the reactions are usually in the range of 70–90% [6], but most of these byproducts remain strongly adsorbed on the catalyst surface, as indicated by the considerable increase in the carbon assay of the catalyst after the first use (ca. 10%) [26]. Typical byproducts are formed by epoxide rearrangement and ring opening [6]. Products involving the oxidation of the allylic position due to radicalar processes were not observed, because the catalyzed epoxidation was carried out with ultra-pure alumina obtained by the sol–gel method [6,11,13,14].

But the question "what is the role of chemisorbed acetate and other organics in alumina catalyzed epoxidation?" may arise. The answer is not straightforward, because the chemisorption of organics has two opposing consequences: (i) poisoning of the labile type Ia Al–OH groups that are involved in the activation of H_2O_2 for epoxidation of nucleophilic olefins by formation of Al–OOH groups [12], and (ii) alteration of the hydrophilic/hydrophobic behavior of the surface, because the increasing hydrophobicity of the surface is what makes the approach of the olefin to the surface easier, thereby allowing the reaction to proceed faster [13,14]. Table 4 provides information on the trends of the carbon assay (determined by elemental analysis) and the pH of the aqueous suspension of catalyst before use (cycle 0) and after use (cycles 1, 3, and 5) to answer this question.

γ-Al_2O_3 has multisite surface Al–OH groups with large differences of acidic strength. According to the Knözinger and Ratnasamy model for the γ-Al_2O_3 surface [27], the hydroxyls at terminal configurations of the surface (types Ia and Ib) are less acidic and more labile, whereas the hydroxyls in bridging configurations (types IIa, IIb, and III) are sluggish and prone

Table 4
Carbon assay and pH of aqueous suspensions (5 wt%) of unused (cycle 0) and used catalyst (cycles 1, 3, and 5)

Cycle	Carbon assay (%)	pH of the catalyst aqueous suspension
0	0.2	7.9
1	3.3	4.6
3	3.4	4.7
5	3.5	4.8

to act as proton donors. For a liquid–solid interface, commonly found in aqueous suspensions of γ-Al_2O_3, estimates indicate that the acidity difference between sites I and III is on the order of 10^8. Regarding the sites Ia and Ib, this difference is also quite high, ca. 10^3 [28,29]. Thus, these labile Al–OH sites can be selectively poisoned during the reaction by adsorption of byproducts, as evidenced by the decrease of the pH of the aqueous suspension of the catalyst before use (7.9, cycle 0) and after use (4.6–4.8, cycles 1, 3, and 5). Moreover, it took 7 h for the pH of an unused catalyst suspension to reach equilibrium, whereas the equilibrium was reached in less than 1 h for the used catalyst samples. This fact also indicates that the unused catalyst has a greater heterogeneity of Al–OH surface sites than the used catalyst.

Recently, we assigned the roles of the different types of Al–OH sites of the alumina/H_2O_2 catalytic system to their activities in epoxidation and H_2O_2 decomposition [12]. H_2O_2 activation on the alumina surface is proposed to occur by reaction of the weak type Ia Brønsted acid sites with H_2O_2, giving the superficial hydroperoxides, Al–OOH, that are responsible for oxygen transfer to the olefin [12,30]. Moreover, we reported that the weakest and more abundant type Ib Al–OH sites have no role in the activation of H_2O_2, because these sites are poisoned by preferential chemisorption of acetate on the alumina surface [12]. However, this site poisoning seems not related to catalytic deactivation, because the use of solvents that are not prone to form carboxylates, such as methanol, isopropanol, and tetrahydrofuran, in the alumina-catalyzed epoxidation of limonene gives much lower conversions than epoxidations carried out in ethyl-acetate or acetonitrile [7].

When the catalyst is recycled, the type Ib sites become less available, and the type Ia Al–OH sites start to be consumed, resulting in decreased catalyst productivity. Because the decomposition of H_2O_2 occurs in parallel on the surface, poisoning of the sites that activate H_2O_2 for epoxidation causes an increase in the consumption of H_2O_2 per epoxide formed, as observed for cycle 5 (Table 1).

Water present in the reaction mixture prolongs the lifetime of the catalyst, because using azeotropic distillation and/or anhydrous H_2O_2 in ethyl acetate does not allow more than three recyclings of the alumina [15]. The role of water in adsorption of organic molecules can be rationalized through the following chemical equilibrium:

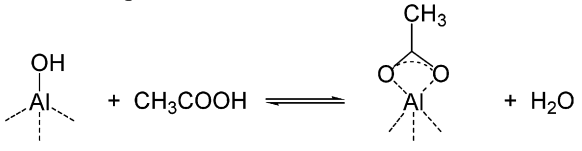

The presence of water in the reaction mixture shifts the chemical equilibrium toward “conservation” of the active sites for epoxidation. Indeed, a band at around 210 nm seen by UV–vis spectroscopy in the aqueous suspension of used catalyst was increased (Fig. 9), possibly due to acetic acid desorption. We estimated the amount of desorbed acetate using the UV absorption at 210 nm. This approach showed that the equivalent carbon assay of the alumina could be as much as 15 wt% for alumina cycle 3. This result contrasts strongly with

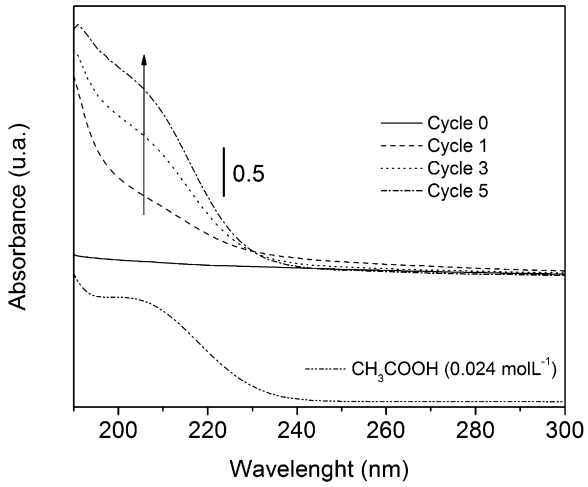

Fig. 9. UV–vis spectra of the aqueous phase from the catalyst suspension (cycles 0, 1, 3, and 5) and of a 0.024 mol L^{-1} acetic acid solution.

the carbon assay determined by elemental analysis (3.4 wt%, Table 4). Moreover, the pH of aqueous acetic acid at an equivalent concentration as that estimated by UV–vis spectroscopy is lower (3.3) than that observed for the aqueous suspension of used catalysts (4.6–4.8; Table 4), indicating that the origin of this discrepancy in the carbon assay is not only the desorbtion of acetic acid, but also the desorption of other molecules, producing the chromophores seen in this UV region. Indeed, direct injection electron-spray ionization mass spectroscopy (ESI-MS) demonstrated that several high-mass ions are present in the aqueous phase of the alumina cycle 3 suspension, which could be oligomers of cyclooctene oxide and mainly acetate-containing aluminum polycations. However, no catalytic reaction occurs after the catalyst is filtered off from the reaction mixture, demonstrating that these water-soluble species are not active for epoxidation.

The chemisorbed molecules (acetate, diols, and oligomers) are strongly bonded to the alumina surface, making them difficult to totally remove by calcination even at 400–500 °C. Typically, alumina recalcined at 400 °C is a yellow or gray solid, indicating the formation of carbonaceous compounds that partially block the alumina surface and thus deactivate the catalyst [11]. In the TG curves of the unused and used catalysts (Figs. 10 and 11), the weight losses between 110 and ca. 300 °C are assigned mainly to the desorption of organic molecules. This is in agreement with the carbon content found by elemental analysis (Table 4). During recalcination, a small but significant fraction of these organic molecules is transformed into surface carbonaceous compounds that can be removed only at higher temperatures (ca. 600 °C; Fig. 11), where the catalyst loses its structural and textural properties necessary for epoxidation [13,14]. The successive increase of weight loss from 15 to 24% for the aluminas of cycle 1 to cycle 5 (Fig. 10) is not directly proportional to the amount of organic material adsorbed on the alumina surface, because the carbon assay is almost steady at ca. 3.5 wt% after the first reaction (Table 4). The increasing weight loss is also likely associated with an increased amount of pseudo-boehmite and amorphous aluminum hydrox-

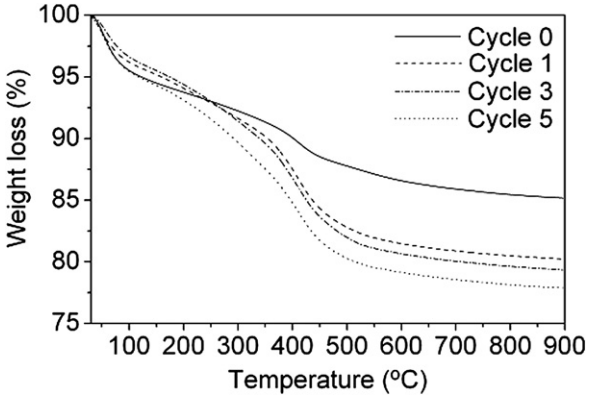

Fig. 10. TG curves for the unused (cycle 0) and used catalyst (cycles 1, 3, and 5).

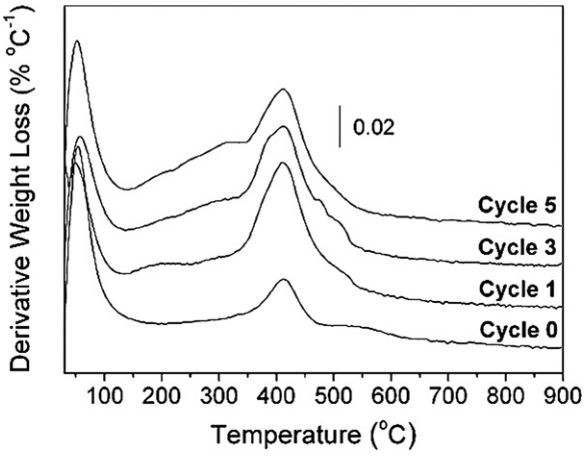

Fig. 11. Derivative TG curves for the unused (cycle 0) and used catalyst (cycles 1, 3, and 5). All curves are in the same scale.

ides formed during catalyst recycling, which are decomposed around 400 °C, giving γ-Al_2O_3, as shown by the increased peak height in the derivative TGA curve (Fig. 11).

4. Conclusion

The deactivation of γ-Al_2O_3 is not straightforward. Some chemical and physical changes associated with the deactivation of the alumina used for catalytic epoxidation with H_2O_2 are attributed to the presence of water in the reaction mixture and to the adsorption of organic molecules on the alumina surface. On the other hand, water plays an important role related to prolonging catalyst lifetime by shifting the equilibria of the adsorption of byproducts. The proposed roles for water in the chemical and physical changes of alumina are as follows:

1. Water causes deleterious changes in the textural properties of the catalyst, such as increasing the population of smaller pores closed at one end (ink bottle-shaped pores). These textural changes decrease the selectivity for highly reactive epoxides, because the residence time of reagents and products inside these pores can be sufficiently long for further oxidation or ring-opening reactions [6]. Moreover, in smaller pores, diffusion of the reagents and products is more problematic.
2. Water causes structural changes in γ-Al_2O_3 due to the formation of less active (oxy)-hydroxides.
3. Water shifts the chemical equilibria of the adsorption of organic molecules (acetic acid, diols, and oligomers) preserving the type Ia Al–OH sites on γ-Al_2O_3, responsible for catalytic epoxidation. However, at higher concentrations, water also makes the approach of hydrophobic olefins to the alumina surface more difficult [13,14].
4. Small amounts of water are needed to minimize H_2O_2 decomposition [5]. Decomposition of H_2O_2 by alumina surfaces is not well understood, but it is clearly related to strong Brønsted acid sites, which may be poisoned by water or other byproducts to some extent [12], thus reducing their activity.

Acknowledgments

The authors are grateful to FAPESP and CNPq for financial support and to Peróxidos do Brasil (Solvay) for supplying the 70 wt% aqueous hydrogen peroxide (Interox 70-10). The authors thank Professor Wanda de Oliveira (IQ/USP) for providing the Raman analyses and Professor Carol Collins for carefully reading the manuscript.

Supplementary material

FTIR spectra (400–4000 cm^{-1}) and Raman spectra of unused catalyst (cycle 0) and used catalyst (cycle 5).

Please visit doi:10.1016/j.jcat.2006.11.011.

References

[1] C.H. Bartholomew, Appl. Catal. A Gen. 212 (2001) 17.
[2] P.G. Menon, Chem. Rev. 94 (1994) 1021.
[3] I.W.C.E. Arends, R.A. Sheldon, Appl. Catal. A Gen. 212 (2001) 175.
[4] R.A. Sheldon, M. Wallau, I.W.C.E. Arends, U. Schuchardt, Acc. Chem. Res. 31 (1998) 485.
[5] M.C.A. van Vliet, D. Mandelli, I.W.C.E. Arends, U. Schuchardt, R.A. Sheldon, Green Chem. 3 (2001) 243.
[6] J.M.S. Silva, F.S. Vinhado, D. Mandelli, U. Schuchardt, R. Rinaldi, J. Mol. Catal. A Chem. 252 (2006) 186.
[7] M.A. Uguina, J.A. Delgado, A. Rodriguez, J. Carretero, D. Gomez-Diaz, J. Mol. Catal. A Chem. 256 (2006) 208.
[8] D. Mandelli, M.C.A. van Vliet, R.A. Sheldon, U. Schuchardt, Appl. Catal. A Gen. 219 (2001) 2001.
[9] V.R. Choudhary, N.S. Patil, N.K. Chaudhari, S.K. Bhargava, J. Mol. Catal. A Chem. 227 (2005) 217.
[10] I.W.C.E. Arends, R.A. Sheldon, Top. Catal. 19 (2002) 133.
[11] R.G. Cesquini, J.M.S. Silva, C.B. Woitiski, D. Mandelli, R. Rinaldi, U. Schuchardt, Adv. Synth. Catal. 344 (2002) 911.
[12] R. Rinaldi, F.Y. Fujiwara, W. Hölderich, U. Schuchardt, J. Catal. 244 (2006) 92.
[13] R. Rinaldi, U. Schuchardt, J. Catal. 236 (2005) 335.
[14] R. Rinaldi, U. Schuchardt, J. Catal. 227 (2004) 109.
[15] R. Rinaldi, J. Sepulveda, U. Schuchardt, Adv. Synth. Catal. 346 (2004) 281.
[16] T. Tsukada, H. Segawa, A. Yasumori, K. Okada, J. Mater. Chem. 9 (1999) 549.
[17] G. Lefevre, M. Duc, P. Lepeut, R. Caplain, M. Fedoroff, Langmuir 18 (2002) 7530.

[18] C. Misra, Industrial Alumina Chemicals, Am. Chem. Soc., Washington, DC, 1986.
[19] B.C. Lippens, Structure and Texture of Aluminas, Ph.D. thesis, Technical University of Delft, The Netherlands, 1961, 178 p.
[20] J.J. Fitzgerald, G.P. Steven, F. Dec, M. Seger, G.E. Maciel, J. Am. Chem. Soc. 119 (1997) 7832.
[21] J.P. Amoureux, C. Fernandez, Solid State Nucl. Magn. Reson. 16 (2000) 339.
[22] M.J. Duer, Introduction to Solid-State NMR Spectroscopy, Blackwell Publishing, Oxford, 2004, p. 235.
[23] U.G. Nielsen, J. Skibsted, H.J. Jakobsen, Chem. Commun. (2001) 2690.
[24] C.C. Landry, N. Pappe, M.R. Mason, A.W. Apblett, A.N. Tyler, A.N. MacInnes, A.R. Barron, J. Mater. Chem. 5 (1995) 331.
[25] H. Wijnja, C.P. Schulthess, Spectrochim. Acta Part A 55 (1999) 861.
[26] J.M.S. Silva, Stereo and site selectivity in the epoxidation of terpenes with alumina obtained by the sol–gel process, M.Sc. Dissertation, Universidade Estadual de Campinas, Brazil, 2005, 82 p.
[27] H. Knönzinger, P. Ratnasamy, Catal. Rev. Sci. Eng. 17 (1978) 31.
[28] M. Trueba, S.P. Trasatti, Eur. J. Inorg. Chem. (2005) 3393.
[29] T. Hiemstra, W.H. Vanriemsdijk, G.H. Bolt, J. Colloid Interface Sci. 133 (1989) 91.
[30] J. Rebek, R. McCready, Tetrahedron Lett. 45 (1979) 4337.